

## Supporting Information

### **Durable Dielectric Switching and Photo-responsivity in a Dion–Jacobson Hybrid Perovskite Semiconductor**

*Peng Wang,<sup>a,b</sup> Xinling Li,<sup>a,b</sup> Huang Ye,<sup>b,d</sup> Qianwen Guan,<sup>b,d</sup> Yifei Wang,<sup>b,d</sup> Yaru Geng,<sup>b</sup> Chengshu Zhang,<sup>b,d</sup> Hang Li,<sup>b,d</sup> and Junhua Luo<sup>\*a,b,c,d</sup>*

<sup>a</sup> College of Chemistry, Fuzhou University, Fuzhou 350116, China

<sup>b</sup> State Key Laboratory of Structure Chemistry, Fujian Institute of Research on the Structure of Matter, Chinese Academy of Sciences, Fuzhou, Fujian, 350002, P. R. China. Email: [jhluo@fjirsm.ac.cn](mailto:jhluo@fjirsm.ac.cn)

<sup>c</sup> Key Laboratory of Fluorine and Silicon for Energy Materials and Chemistry of Ministry of Education, School of Chemistry and Chemical Engineering, Jiangxi Normal University, Nanchang, Jiangxi 330022, China.

<sup>d</sup> University of Chinese Academy of Sciences, Beijing, 100049, China.

## Experimental Section

**Materials:** Lead (II) acetate trihydrate ( $\text{Pb}(\text{AC})_2 \cdot 3\text{H}_2\text{O}$ , 99.5%, AR), hydrobromic acid (HBr, 48%), 1,4-butanediamine (BDA, 98%), methylamine (MA, 30% in  $\text{H}_2\text{O}$ ) are used as received from Aladdin without further purification.

**Synthesis and crystal growth:** MA (5 mmol, 0.4g) and  $\text{Pb}(\text{Ac})_2 \cdot 3\text{H}_2\text{O}$  (10 mmol, 3.67 g) were dissolved in 20 ml of hydrobromic acid with stirring for 10 minutes at room temperature. Then 1,4-butanediamine (10 mmol, 0.810g) was added to the mixed solution until the precipitate was completely dissolved by heating. The yellow transparent crystals of **1** were obtained after 24 h. Meanwhile, bulk single crystals were grown by the temperature-cooling method from its saturated solution at a rate of  $0.2 \text{ K d}^{-1}$ .

**Single crystal structure determination and Powder X-ray diffraction:** Single crystal X-ray diffraction (XRD) experiments were performed on a Bruker APEX-II diffractometer with Mo  $K\alpha$  radiation, operating at 50 kV and 40 mA. The structures were solved by direct method and refined by full-matrix least-squares on F2 using the SHELX package. The structure-solving and refinement processes were conducted in the Olex2 software. Powder X-ray diffraction (PXRD) data was obtained by Rigaku Miniflex600 powder X-ray diffractometer with the  $2\theta$  range of  $5^\circ$ - $50^\circ$  at room temperature.

**Thermal analyses:** The thermogravimetric analysis data were obtained by using Mettler Toledo TGA/SDTA 851e. Differential scanning calorimetry (DSC) analysis was performed on NETZSCH DSC 200 F3 equipment within the temperature range of 250-375 K. The measurement was performed in a nitrogen atmosphere with a scanning rate of  $10 \text{ K min}^{-1}$ .

**Dielectric constant measurements:** The pressed-powder pellets and bulk crystals coated with silver conduction paste of **1** were employed for the dielectric experiments. The TH2828A Precision LCR meter was used to conduct the variable-temperature dielectric measurements within the respective frequency of 10 kHz, 100 kHz, 300 kHz, 500 kHz, and 1000 kHz, and the temperature range of 235–350 K.

**UV–Vis–NIR Diffuse Reflectance Spectroscopy:** UV-vis diffuse reflectance spectra of desired materials were performed at room temperature on Perkin-Elmer Lambda 900 UV-vis spectrophotometer in the variable wavelength range between 250 to 800 nm. The anhydrous BaSO<sub>4</sub> powder was used as the 100% reflectance reference, and the powdered crystal was used for the measurements.

**Computational description:** The crystal structural data at LTP of **1** was used for the first-principles density functional theory (DFT) calculations. Partial density of states (PDOS) and band structure were calculated by the total-energy code CASTEP. Under the generalized gradient approximation, the Kleinman-Bylander form of norm-conserving pseudopotentials was employed to model interactions between ionic cores and electrons. The high cut-off energy of 820 eV and the k-point sampling of the Brillouin zone of  $2 \times 2 \times 1$  were set for **1**, respectively. The following orbital electrons were treated as valence electrons: Pb  $6s^26p^2$ , Br  $4s^24p^5$ , C  $2s^22p^2$ , N  $2s^22p^3$ , and H  $1s^1$ .

**Photodetection property measurements:** The temperature-dependent conductivity of **1** was measured along the *a*-, *b*-, and *c*-axis crystal direction ranging from 300 to 400 K. During photoelectric measurement, the *I-V* curves of the detectors were measured under the light of 405 nm. (LP405-MF300) serves as the light source, and a PM100D optical power meter is used to measure the light intensity. A Keithley 6517B source meter was installed on the device and the photo-response was measured in the visible light range at room temperature. The response time was recorded using a high-speed Tektronix DS1052E oscilloscope.

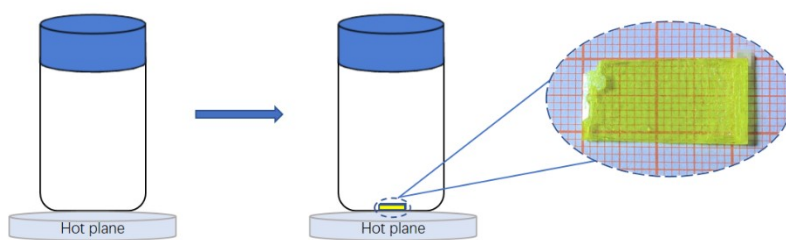


Fig S1. A schematic showing the growth of single crystals.

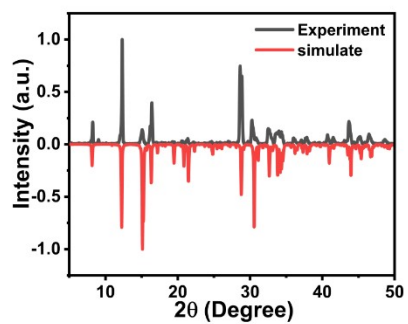


Fig S2. Experimental and simulated powder X-ray diffraction patterns for **1**.

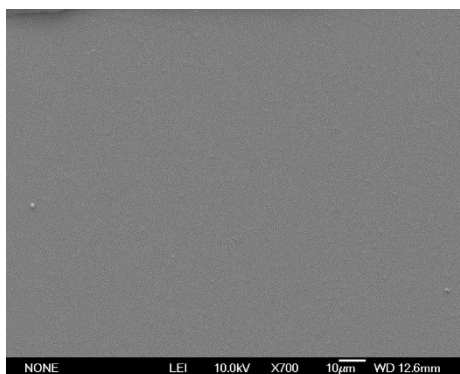


Fig S3. SEM image of **1**.

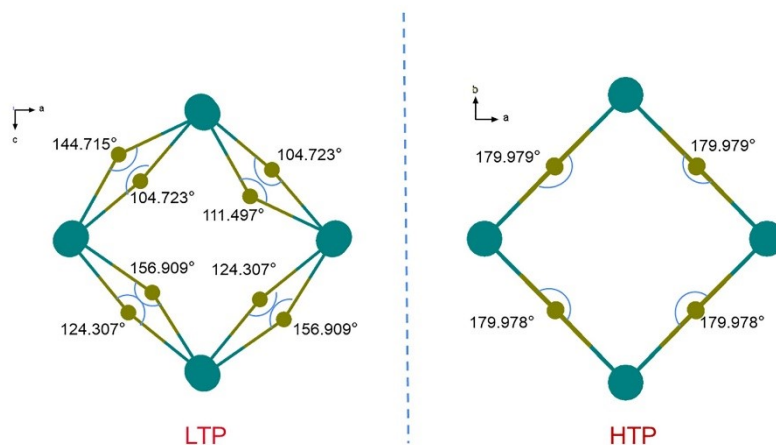


Fig S4. The equatorial angles of the inorganic layer in **1**.

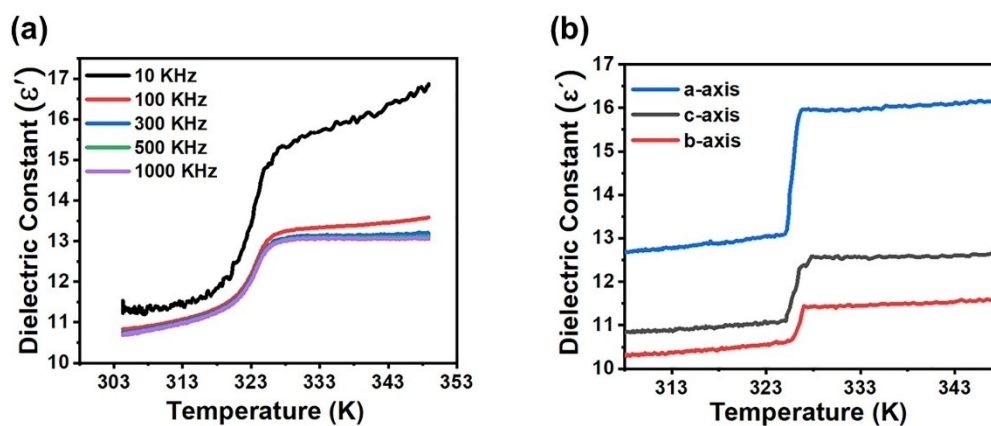


Fig S5. (a) The dielectric constant curves of **1** under different frequency. (b) Dielectric constants curves of **1** measured along the *a*-, *b*- and *c*-axis at 1000 KHz.

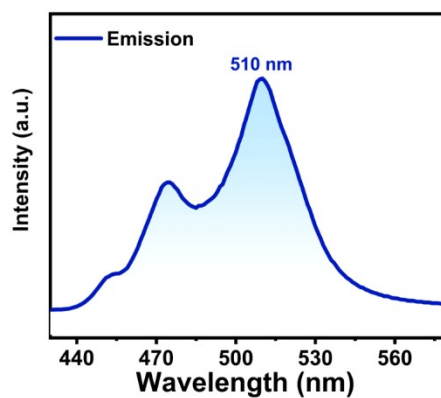


Fig S6. PL spectra of **1**.

**Table S1.** Crystal data and structure refinements for **1** collected at LTP and HTP.

Empirical formula	C <sub>6</sub> H <sub>26</sub> Br <sub>10</sub> N <sub>4</sub> Pb <sub>3</sub>	C <sub>6</sub> H <sub>26</sub> Br <sub>10</sub> N <sub>4</sub> Pb <sub>3</sub>
Formula weight	1574.98	1574.98
Temperature [K]	297.34(10)	343.02
Crystal system	orthorhombic	orthorhombic
Space group (number)	<i>Pnma</i>	<i>Cmcm</i>
<i>a</i> [Å]	8.3682(5)	8.3213(4)
<i>b</i> [Å]	43.331(3)	8.4780(6)
<i>c</i> [Å]	8.3003(5)	42.894(3)
$\alpha$ [°]	90	90
$\beta$ [°]	90	90
$\gamma$ [°]	90	90
Volume [Å <sup>3</sup> ]	3009.7(3)	3026.1(3)
<i>Z</i>	4	4
$\rho_{\text{calc}}$ [gcm <sup>-3</sup> ]	3.476	3.457
$\mu$ [mm <sup>-1</sup> ]	30.018	29.855
<i>F</i> (000)	2744.0	2744.0
Radiation	Mo <i>K</i> <sub>α</sub> (λ=0.71073 Å)	Mo <i>K</i> <sub>α</sub> (λ=0.71073 Å)
2θ range [°]	4.996 to 60.894	7.12 to 55.006
Index ranges	-8 ≤ <i>h</i> ≤ 11, -54 ≤ <i>k</i> ≤ 45, -10 ≤ <i>l</i> ≤ 10	-10 ≤ <i>h</i> ≤ 10, -11 ≤ <i>k</i> ≤ 10, -55 ≤ <i>l</i> ≤ 55
Reflections collected	15044	12113
Independent reflections	3702 [R <sub>int</sub> = 0.0686, R <sub>sigma</sub> = 0.0521]	1879 [R <sub>int</sub> = 0.0658, R <sub>sigma</sub> = 0.0504]
Data/restraints/parameters	3702/0/113	1879/40/90
Goodness-of-fit on <i>F</i> <sup>2</sup>	1.077	1.107
Final <i>R</i> indexes [ <i>I</i> ≥ 2σ ( <i>I</i> )]	R <sub>1</sub> = 0.0611, wR <sub>2</sub> = 0.1450	R <sub>1</sub> = 0.0592, wR <sub>2</sub> = 0.1697
Final <i>R</i> indexes [all data]	R <sub>1</sub> = 0.0803, wR <sub>2</sub> = 0.1562	R <sub>1</sub> = 0.0791, wR <sub>2</sub> = 0.1851
Largest diff. peak/hole / e Å <sup>-3</sup>	2.31/-3.37	2.87/-2.72

**Table S2.** The bond lengths of **1** at LTP and HTP.

	LTP		HTP
Pb1–Br6	2.8415(14)	Pb1–Br2 <sup>#1</sup>	2.954(3)
Pb1–Br4 <sup>#1</sup>	2.9755(13)	Pb1–Br2	2.954(3)
Pb1–Br4	2.9716(14)	Pb1–Br1	2.973(3)
Pb1–Br5 <sup>#2</sup>	2.9877(14)	Pb1–Br1 <sup>#2</sup>	2.967(3)
Pb1–Br5	2.9797(13)	Pb1–Br1 <sup>#3</sup>	2.967(3)
Pb1–Br3	3.1531(14)	Pb1–Br1 <sup>#4</sup>	2.973(3)
Pb2–Br1 <sup>#3</sup>	3.0730(19)	Pb2–Br2	3.093(3)
Pb2–Br1	3.0649(19)	Pb2–Br3	2.969(2)
Pb2–Br2 <sup>#2</sup>	2.986(2)	Pb2–Br3 <sup>#5</sup>	2.971(2)
Pb2–Br2	2.9924(19)	Pb2–Br3 <sup>#6</sup>	2.9695(19)
Pb2–Br3	2.9682(13)	Pb2–Br3 <sup>#3</sup>	2.971(2)
Pb2–Br3 <sup>#4</sup>	2.9682(13)	Pb2–Br4	2.868(4)

**Table S3.** The bond angles of **1** at LTP.

Atom–Atom–Atom	Angle [°]	Atom–Atom–Atom	Angle [°]
Br6–Pb1–Br4	89.51(5)	Br2–Pb2–Br1	172.78(6)
Br6–Pb1–Br4	87.34(5)	Br2–Pb2–Br1	178.06(6)
Br6–Pb1–Br5	90.75(5)	Br2–Pb2–Br2	93.16(2)
Br6–Pb1–Br5	88.35(5)	Br3–Pb2–Br1	91.34(4)
Br6–Pb1–Br3	167.97(5)	Br3–Pb2–Br1	85.74(3)
Br4–Pb1–Br4	89.862(13)	Br3–Pb2–Br1	85.74(3)
Br4–Pb1–Br5	177.74(5)	Br3–Pb2–Br1	91.34(4)
Br4–Pb1–Br5	89.32(5)	Br3–Pb2–Br2	94.21(3)
Br4–Pb1–Br5	91.43(5)	Br3–Pb2–Br2	88.13(4)
Br4–Pb1–Br5	177.69(5)	Br3–Pb2–Br2	88.13(4)
Br4–Pb1–Br3	82.36(5)	Br3–Pb2–Br2	94.21(3)
Br4–Pb1–Br3	84.27(4)	Br3–Pb2–Br3	170.97(7)
Br5–Pb1–Br5	89.324(14)	Pb2–Br1–Pb2	158.24(8)
Br5–Pb1–Br3	99.67(5)	Pb2–Br2–Pb2	149.08(9)
Br5–Pb1–Br3	97.70(5)	Pb1–Br4–Pb1	164.34(7)
Br1–Pb2–Br1	87.892(19)	Pb1–Br5–Pb1	162.12(7)
Br2–Pb2–Br1	94.05(6)		

**Table S4.** The bond angles of **1** at HTP.

Atom–Atom–Atom	Angle [°]	Atom–Atom–Atom	Angle [°]
Br2–Pb1–Br2	179.94(17)	Br3–Pb2–Br2	90.13(9)
Br2–Pb1–Br1	89.98(6)	Br3–Pb2–Br2	90.13(9)
Br2–Pb1–Br1	90.02(6)	Br3–Pb2–Br3	178.50(13)
Br2–Pb1–Br1	89.98(6)	Br3–Pb2–Br3	91.067(5)
Br2–Pb1–Br1	90.02(6)	Br3–Pb2–Br3	87.59(11)
Br2–Pb1–Br1	89.98(6)	Br3–Pb2–Br3	90.26(11)
Br2–Pb1–Br1	90.02(6)	Br3–Pb2–Br3	178.50(13)
Br2–Pb1–Br1	89.98(6)	Br3–Pb2–Br3	91.067(5)
Br2–Pb1–Br1	90.02(6)	Br4–Pb2–Br2	168.91(9)
Br1–Pb1–Br1	91.069(5)	Br4–Pb2–Br3	79.38(10)
Br1–Pb1–Br1	179.78(16)	Br4–Pb2–Br3	99.85(11)
Br1–Pb1–Br1	91.069(5)	Br4–Pb2–Br3	93.47(10)
Br1–Pb1–Br1	179.78(17)	Br4–Pb2–Br3	86.10(10)
Br1–Pb1–Br1	88.71(16)	Pb1–Br2–Pb2	179.67(16)
Br1–Pb1–Br1	89.15(16)	Pb1–Br1–Pb1	179.78(16)
Br3–Pb2–Br2	90.56(8)	Pb2–Br3–Pb2	178.50(13)
Br3–Pb2–Br2	90.56(9)		